

Bound states induced by a ferromagnetic delta-layer inserted into a three-dimensional topological insulator

V. N. Men'shov¹), V. V. Tugushev, E. V. Chulkov⁺

National Research Centre "Kurchatov Institute", 123182 Moscow, Russia

Tomsk State University, 634050 Tomsk, Russia

⁺Departamento de Física de Materiales, Facultad de Ciencias Químicas, UPV/EHU and Centro de Física de Materiales CFM-MPC, Centro Mixto CSIC-UPV/EHU, Apdo. 1072, 20080 San Sebastián, Basque Country, Spain

Submitted 17 August 2012

We report on theoretical study of the bound electron states induced by a ferromagnetic delta-layer embedded into a narrow-band-gap semiconductor of the Bi_2Se_3 -type which is a three-dimensional topological insulator with large spin-orbit coupling. We make use of an effective Hamiltonian taking into account the inverted band structure of the semiconductor host at the Γ point and describe the properties of the in-gap bound states: energy spectrum, characteristic length and spin polarization. We highlight a role of these states for a magnetic proximity effect in digital magnetic heterostructures based on the Bi_2Se_3 -type semiconductors.

1. Introduction. Since the discovery of three-dimensional (3D) topological insulators (TIs), interplay between topological order and magnetism has been considered as one of the field of paramount importance [1, 2]. When time-reversal symmetry is broken, topological surface states are expected to exhibit a wide range of exotic spin phenomena (for example, quantized anomalous Hall effect) [3–5] which are potentially useful for spintronic applications [6]. The spontaneous symmetry breaking in the system can be realized by the doping with magnetic ions to induce magnetism in the bulk or on the surface of TI [7–9], or by a heterostructure design wherein exchange field is induced at the TI surface by the quantum proximity to a ferromagnetic (FM) material [9, 10]. However, there is one more way to create magnetization in TI, which is still out of the activity field of both experimentalists and theorists. Keeping in mind the fact that the modern molecular beam epitaxy technology makes it possible to prepare digital magnetic heterostructures (DMHs) in which mono- (submono)-layers of transition metals, embedded into the semiconductor TI host, form the so-called FM delta-layers (δ layers) [11]. In this work, we explore theoretically how the electron and spin densities of a 3D TI host are affected by an inserted FM δ layer.

A common manner to introduce ferromagnetism into TI is the doping with transition metal impurities, just as that has been succeeded in diluted magnetic semiconductors (DMSs) [12]. The thin films of TI DMS $\text{Sb}_{2-x}\text{Cr}_x\text{Te}_3$ [13] and $\text{Sb}_{2-x}\text{V}_x\text{Te}_3$ [14] display robust, out-of-plane FM order with the Curie temperature in-

creasing almost linearly with the content of 3d impurity, so that the highest Curie temperatures are 190 K in a $\text{Sb}_{1.41}\text{Cr}_{0.59}\text{Te}_3$ film and 177 K in a $\text{Sb}_{1.65}\text{V}_{0.35}\text{Te}_3$ film. Just recently, Salman et al. [15] have found that even at Fe doping levels as low as 5 percent, the full volume of $\text{Bi}_{2-x}\text{Fe}_x\text{Se}_3$ becomes magnetic at a relatively high temperature of ~ 250 K.

As it is well known, DMSs are characterized by a strong disorder in the distribution of the magnetic metal atoms in the host; as a result, the large content of 3d dopant in the TI DMSs influences their band structure so that topological order may be lost due to a strong exchange scattering. In contrast, it is generally thought that, in the epitaxial growth process of the Bi_2Se_3 -type based DMHs, the diffusion smearing and roughness of the FM δ layers are restricted within a relevant quintuple. At the same time, the FM order in the layers, enriched in 3d transition metal (Cr, V, Fe) atoms and embedded into the TI host (Sb_2Te_3 , Bi_2Se_3), could manifest itself at the temperatures well above a room temperature.

Below we consider the model of a single FM δ layer embedded into the 3D TI host of the Bi_2Se_3 -type semiconductor with an inverted band gap, described on the basis of the $\mathbf{k} \cdot \mathbf{p}$ Hamiltonian [16]. Strictly speaking, the very assumption that the FM order exists inside the δ layer is not evident [17], but in our model, this order promoted by strong correlations of electron states at the transition metal ions is merely postulated. The influence of the FM δ layer on the electron states of the TI host is described by means of an effective one-dimensional potential, which includes both a potential (spin-independent) and an exchange (spin-dependent)

¹) e-mail: vnmenshov@mail.ru

contribution. We argue that the FM δ layer induces the quasi-2D bound electron states residing inside a TI host gap. Within the framework of a continual approach, we study these states to determine their energy spectrum, spin polarization, space shape, and characteristic length λ . In this letter we concentrate only on the key aspects of the phenomenon omitting many cumbersome calculation details.

2. Model Hamiltonian. We begin considering the model $\mathbf{k} \cdot \mathbf{p}$ Hamiltonian for materials of the Bi_2Se_3 -family [16]:

$$H_h = \int d\mathbf{r} \psi^\dagger(\mathbf{r}) E^{(\mathbf{k} \cdot \mathbf{p})} (-i\nabla) \psi(\mathbf{r}), \quad (1)$$

where $\psi(\mathbf{r})$ is the smooth envelope function in the spinor basis ($|+, \uparrow\rangle, |-, \uparrow\rangle, |+, \downarrow\rangle, |-, \downarrow\rangle$) of the four low-lying states at the Γ point with $\mathbf{k} = 0$. The signs “ \pm ” denote the even and odd parity states, respectively, and the arrows $\uparrow\downarrow$ indicate the spin projections. In the Bi_2Se_3 -type material, these four states originate from the bonding combinations of Bi P_{1z} -orbitals and anti-bonding combinations of Se P_{2z} -orbitals. The important symmetries of the system are time-reversal symmetry T , inversion symmetry I and three-fold rotation symmetry C_3 along the z -axis. Keeping only the terms up to quadratic order in the wave vector \mathbf{k} , Zhang et al. constructed the following generic form of the 4×4 effective Hamiltonian [16]:

$$E^{(\mathbf{k} \cdot \mathbf{p})}(\mathbf{k}) = \varepsilon_0(\mathbf{k}) \mathbf{I}_{4 \times 4} + \Xi(\mathbf{k}) \tau_z \sigma_0 + A_{\parallel} \tau_x (k_x \sigma_x + k_y \sigma_y) + A_z k_z \tau_z \sigma_z, \quad (2)$$

with $\Xi(\mathbf{k}) = \Xi - B_{\parallel}(k_x^2 + k_y^2) - B_z k_z^2$; $\mathbf{I}_{4 \times 4}$ is a unit matrix, $\sigma_{0,x,y,z}$ and $\tau_{0,x,y,z}$ denote the Pauli matrices in the spin and orbital space, respectively. An important feature is that the orbitals $|+, \uparrow\rangle$ ($|\downarrow\rangle$) and $|-, \uparrow\rangle$ ($|\downarrow\rangle$) at the Γ point have the opposite parities, so that the off-diagonal terms are linear in $k_{x,y}$ and k_z . The simple model (1), (2) captures remarkable features of the band structure, especially, under the condition Ξ , B_z , $B_{\parallel} > 0$, the inverted order of the terms $|+, \uparrow\rangle$ ($|\downarrow\rangle$) and $|-, \uparrow\rangle$ ($|\downarrow\rangle$) near $\mathbf{k} = 0$ (as compared with large \mathbf{k}), which correctly characterizes the topologically non-trivial nature of the system due to the strong spin orbit coupling. In what follows, for simplicity we assume $\varepsilon_0(\mathbf{k}) = 0$ and $B_z = B_{\parallel} = B$ and $A_z = A_{\parallel} = A$. Then the dispersion of the bulk bands is given by $\omega = \pm\omega_0(\mathbf{k})$ with $\omega_0(\mathbf{k}) = \sqrt{\Xi^2(\mathbf{k}) + A^2 k^2}$, $k^2 = k_x^2 + k_y^2 + k_z^2$. We restrict ourselves to the case of “camelback” shaped bands ($2B\Xi > A^2$) when the band gap gets the minimal magnitude $E_g = 2\Omega$ at the nonzero wave-vector $k = k_0$, where $k_0 = \frac{\sqrt{2B\Xi - A^2}}{\sqrt{2B}}$, $\Omega = \omega_0(k_0) = \frac{A\sqrt{4B\Xi - A^2}}{2B}$.

The model Hamiltonian (1), (2) is defined on the whole space of the host. Although the $\mathbf{k} \cdot \mathbf{p}$ approach is an efficient tool for the small-momentum realm $ka \ll 1$ (a is the lattice constant), it cannot provide adequate information on the wave-function behavior in the vicinity of the atomically sharp FM δ layer where large momenta are highly important. The embedding of the FM δ layer drastically perturbs the electron density and deforms the crystal lattice of the host. In fact, the internal electron properties of the TI host near the FM δ layer may significantly differ from those at the periphery of this layer. Therefore, assuming the FM δ layer to be located at $z = 0$ and retaining a 2D periodicity along the (x, y) plane, we introduce the Hamiltonian $H_{\delta} = a \int d\mathbf{r} \psi^\dagger(\mathbf{r}) Y(z) \psi(\mathbf{r})$ of the FM δ layer perturbing the electron states of the TI host. In principle, the effective spin-dependent potential $Y(z) = \varphi(z) + U(z)$ contains components with different spatial scales. The long-range component $\varphi(z)$ caused by the charge redistribution around the δ layer induces the energy band bending deep into the TI host (really, on the scale of tens of nanometers in the Bi_2Se_3 -type non-degenerate semiconductors). The scale of the short-range component $U(z)$ is of the order of the δ layer thickness and may reach several angstroms in the advanced selective doping technologies. For simplicity, we include the long-range component $\varphi(z)$ into the renormalization of the chemical potential of the system, while the short-range component $U(z)$ is treated as a single plane defect described in the phenomenological way by means of a spin-dependent contact potential $U(z) = U\delta(z)$, where

$$U = (V\sigma_0 + \Delta\sigma_z)\tau_0 + (v\sigma_0 + \eta\sigma_z)\tau_z. \quad (3)$$

The matrix elements V , v and Δ , η are related to the processes of potential and exchange scattering, respectively. For the sake of simplicity, we neglect the inter-band scattering processes and imply that the magnetization of the FM δ layer is directed along the normal to its plane.

One can intuitively interpret the physical meaning of the matrix elements of the potential (3). The terms V and v are responsible, respectively, for the symmetric and antisymmetric local shifts (around the middle of the gap $\omega = 0$) of the valence and conduction bands due to Coulomb potential of the δ layer. On the other hand, the terms Δ and η involve, respectively, the symmetric and antisymmetric local spin splitting of the valence and conduction bands produced by an exchange field of the FM δ layer. The quantity and sign of the matrix elements depend, in a complicated manner, on many factors: the sort and concentration of impurity atoms composing the

δ layer; which of the sub-lattices, Bi or Se, is substituted with impurity atoms; etc.

The in-gap bound states of the Hamiltonian $H = H_h + H_\delta$ (1)–(3) can be characterized by the envelope function $\psi(\boldsymbol{\kappa}, z)$ that depends on the longitudinal two-dimensional wave-vector $\boldsymbol{\kappa} = (k_x, k_y)$ (in a plane geometry, the wave-vector $\boldsymbol{\kappa}$ is a good quantum number) and exponentially decays in the directions perpendicular to the δ layers as $\psi(\boldsymbol{\kappa}, z) \sim \exp[-|z|/\lambda(\boldsymbol{\kappa})]$, at $|z| \gg \lambda(\boldsymbol{\kappa})$, where $\lambda(\boldsymbol{\kappa})$ is a decay length.

Within the continual approach, it is quite relevant to make use a variational treatment for the energy functional $F\{\psi^+, \psi\} = H_h + \int d\mathbf{r} \psi^+(\mathbf{r})[U\delta(z) - E]\psi(\mathbf{r})$ that is defined on the whole space, $\psi(\mathbf{r})$ belongs to the set of continuous functions, E is the Lagrange multiplier. Varying functional $F\{\psi^+, \psi\}$ with respect to the function ψ^+ ($\delta F/\delta\psi^+ = 0$) yields the Schrödinger equation for the TI host at $z \neq 0$,

$$E^{(\mathbf{k}\cdot\mathbf{p})}(\boldsymbol{\kappa}, -i\partial/\partial z)\psi(\boldsymbol{\kappa}, z) = E(\boldsymbol{\kappa})\psi(\boldsymbol{\kappa}, z), \quad (4)$$

and imposes the constraint condition at the δ layer,

$$\begin{aligned} B\sigma_0\tau_z \left[\frac{\partial\psi(\boldsymbol{\kappa}, z)}{\partial z} \Big|_{z=0+} - \frac{\partial\psi(\boldsymbol{\kappa}, z)}{\partial z} \Big|_{z=0-} \right] = \\ = U\psi(\boldsymbol{\kappa}, z) \Big|_{z=0}. \end{aligned} \quad (5)$$

It is not difficult to see that Eqs. (4), (5) are satisfied by either an even function $\psi^{(s)}(\boldsymbol{\kappa}, z) = \psi^{(s)}(\boldsymbol{\kappa}, -z)$ (symmetric bound state) or an odd function $\psi^{(A)}(\boldsymbol{\kappa}, z) = -\psi^{(A)}(\boldsymbol{\kappa}, -z)$ (antisymmetric bound state). The even function has a discontinuity in the first derivative at the point $z = 0$ proportional to the potential strength, while the odd function and its first derivative are continuous at $z = 0$. Hence it follows that the energy spectrum and space distribution of the symmetric bound state must directly depend on the spin and orbital structure and the strength of the effective potential of the δ layer. On the other hand, the antisymmetric bound state is insensitive to the details of the effective potential; in essence, this potential just fixes the zero point of the envelope function at the δ layer so that $\psi^{(A)}(\boldsymbol{\kappa}, 0) = 0$.

3. Symmetric bound states at the δ FM layer.

In Ref. [18], within a single-band model, the formalism of an effective potential has been applied to qualitatively explain the effect of induced spin polarization in topologically trivial semiconductor with an inserted FM δ layer. It has been shown that charge and spin densities in the semiconductor host are strongly perturbed due to the effective potential of the δ layer that leads to appearance of the bound states which reside inside the bulk semiconductor gap. In Ref. [18] these states were

called “confinement states” since they are spatially confined near the δ layer. Here, we generalize the formalism of Ref. [18] to study the in-gap bound states induced by the δ layer embedded into the inverted band gap semiconductor host described by the Hamiltonian H_h (1), (2). Having defined the Green's function of the bulk Hamiltonian H_h (1), (2) as $\overset{\circ}{G}(\omega) = [\omega - H_h]^{-1}$, one can straightforwardly write the single-particle Green's function for the Hamiltonian $H = H_h + H_\delta$ (1)–(3) in the momentum representation

$$\begin{aligned} G(\mathbf{k}, \mathbf{k}'; \omega) = (2\pi)^3 \delta(\mathbf{k} - \mathbf{k}') \overset{\circ}{G}(\mathbf{k}; \omega) + \\ + (2\pi)^2 \delta(\boldsymbol{\kappa} - \boldsymbol{\kappa}') \overset{\circ}{G}(\boldsymbol{\kappa}; \omega) T(\boldsymbol{\kappa}; \omega) \overset{\circ}{G}(\boldsymbol{\kappa}'; \omega), \end{aligned} \quad (6)$$

where $T(\boldsymbol{\kappa}; \omega) = U[1 - \overset{\circ}{G}(\boldsymbol{\kappa}; \omega)U]^{-1}$ is the full t matrix for the scattering of electrons on the plane defect potential (3), $\overset{\circ}{G}(\boldsymbol{\kappa}; \omega) \equiv \overset{\circ}{G}(\boldsymbol{\kappa}, z = 0; \omega) = \int \frac{adk_z}{2\pi} \overset{\circ}{G}(\mathbf{k}; \omega)$, $\delta(\mathbf{k})$ is a delta-function. The poles of the t matrix determine the sub-band spectrum $\omega = \omega_i^{(s)}(\boldsymbol{\kappa})$ of the symmetric bound (confinement) state induced by the δ layer. After some algebra one can obtain the set of equations describing the spectrum for the various parameters of the potential (3):

$$\begin{aligned} [1 - V_1 g_1(\boldsymbol{\kappa}; \omega)][1 - V_2 g_2(\boldsymbol{\kappa}; \omega)] - \\ - V_1 V_2 f_1(\boldsymbol{\kappa}; \omega) f_2(\boldsymbol{\kappa}; \omega) = 0, \\ [1 - V_3 g_1(\boldsymbol{\kappa}; \omega)][1 - V_4 g_2(\boldsymbol{\kappa}; \omega)] - \\ - V_3 V_4 f_1(\boldsymbol{\kappa}; \omega) f_2(\boldsymbol{\kappa}; \omega) = 0, \end{aligned} \quad (7)$$

$$\begin{aligned} V_{1,2} = V \pm \Delta \pm v + \eta, \quad V_{3,4} = V \pm \Delta \mp v - \eta, \\ g_{1,2}(\boldsymbol{\kappa}; \omega) = \frac{\pm a}{4B\kappa_+(\boldsymbol{\kappa}; \omega)} \left[1 - \frac{\Xi(\boldsymbol{\kappa}) \pm \omega}{\sqrt{\omega_0^2(\boldsymbol{\kappa}) - \omega^2}} \right], \\ f_{1,2}(\boldsymbol{\kappa}; \omega) = \frac{-a}{4B\kappa_+(\boldsymbol{\kappa}; \omega)} \frac{Ak_\pm}{\sqrt{\omega_0^2(\boldsymbol{\kappa}) - \omega^2}}, \end{aligned} \quad (8)$$

where $\kappa_\pm(\boldsymbol{\kappa}; \omega) = \sqrt{\sqrt{\omega_0^2(\boldsymbol{\kappa}) - \omega^2} \pm B(\kappa^2 - k_0^2)}/\sqrt{2B}$, $\omega_0(\boldsymbol{\kappa}) = \sqrt{\Xi^2(\boldsymbol{\kappa}) + A^2\kappa^2}$, $\Xi(\boldsymbol{\kappa}) = \Xi - B\kappa^2$. Equations (7), (8) are invariant under the simultaneous permutations $\omega \leftrightarrow -\omega$ and $[V + \Delta \pm (v + \eta)] \leftrightarrow -[V - \Delta \mp (v - \eta)]$. At the Γ point ($\boldsymbol{\kappa} = 0$), Eqs. (7) are decoupled to form four independent equations corresponding to spin-polarized bound states of electrons and holes. The energy position of the sub-band edge $\omega_i^{(s)}(0) = \omega_i^{(s)}(\boldsymbol{\kappa} = 0)$, $i = 1, 2, 3, 4$ depends on the strength V_i . Given the parameters V, Δ, v, η , in the general case, the strength V_i takes four different values. As illustrated in Fig. 1, for any magnitude and sign of V_i there always exists a single bound state $\omega_i^{(s)}(0)$. If $V_i > 0$

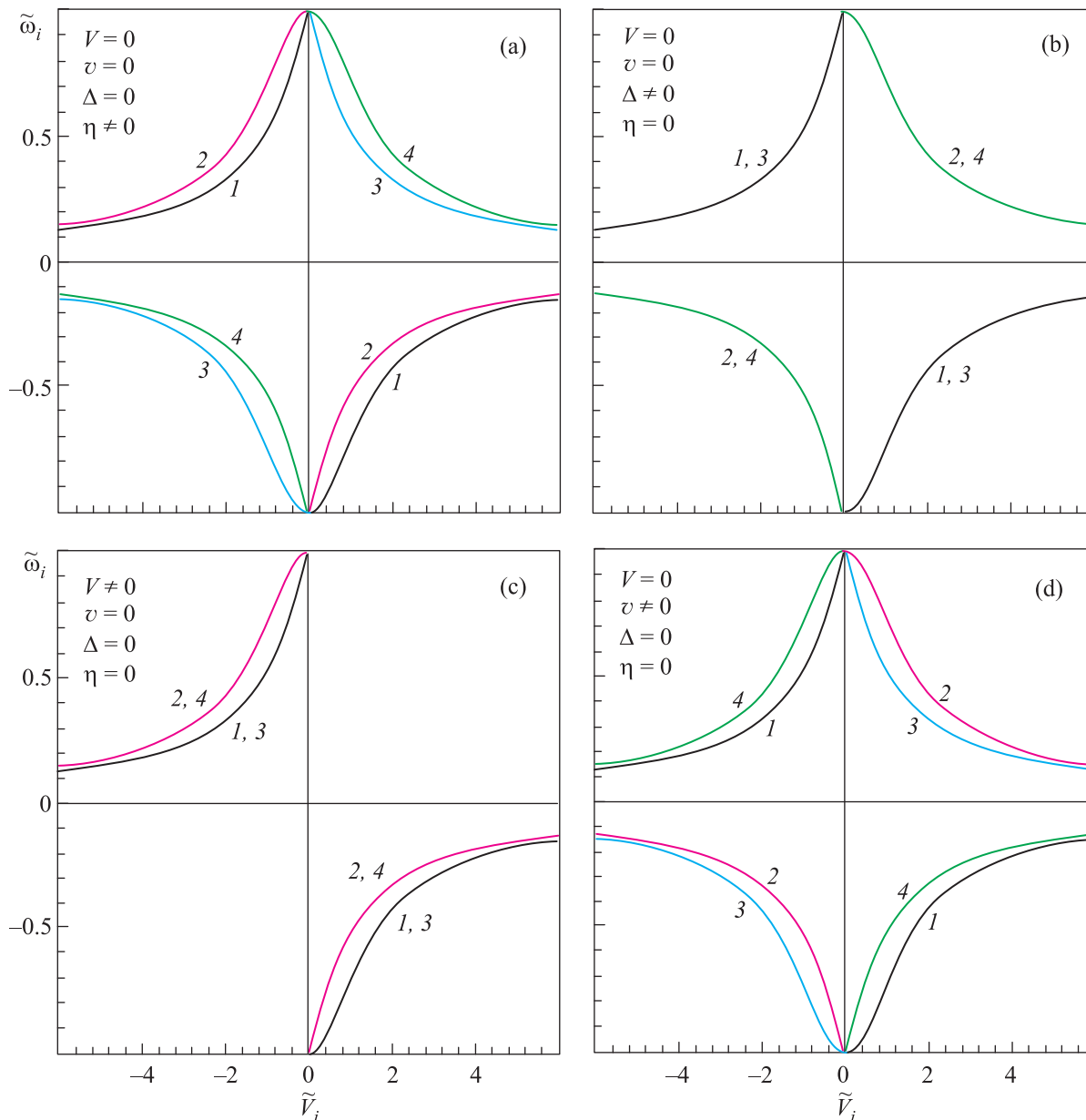


Fig. 1. (Color online) The energy edge of the in-gap bound state as the function of the effective potential strength of the δ layer in the regime $2B\Xi > A^2$ (for concreteness $(A^2/B\Xi) = 1$) for four different partial situations. The variables are measured in the dimensionless units: $\tilde{\omega}_i = \omega_i^{(s)}(0)/\Omega$ and $\tilde{V}_i = aV_i/\sqrt{2B\Xi}$. According to Eq. (8), the letter i indicates the confinement mode $\omega_i^{(s)}(0)$ induced by the potential strength V_i . Each mode is depicted by own color: 1 – black; 2 – red; 3 – blue; 4 – green. In the situations $V \neq 0, v = 0, \Delta = 0, \eta = 0$ and $V = 0, v = 0, \Delta \neq 0, \eta = 0$, where $\omega_1^{(s)}(0) = \omega_3^{(s)}(0)$ and $\omega_2^{(s)}(0) = \omega_4^{(s)}(0)$, the black and red curves merge with the blue and green curves, respectively

$(V_i < 0)$ the corresponding sub-band edge is placed inside the negative (positive) region of the band gap, $-\Omega < \omega_i^{(s)}(0) < 0$ ($0 < \omega_i^{(s)}(0) < \Omega$). Notice that $\omega_i^{(s)}(0|V_i) \neq -\omega_i^{(s)}(0|-V_i)$ at finite value of V_i . Remarkably, under the influence of the effective potential terms V or Δ , the relevant confinement state remains double degenerate.

Omitting detailed derivation, we present the spatial behavior of the envelop function corresponding to i -th confinement mode in the form:

$$\begin{aligned}
 \psi_i^{(s)}(\boldsymbol{\kappa}, z) \sim & \{ \alpha(\boldsymbol{\kappa}) \cos[\kappa_-(\boldsymbol{\kappa}, \omega_i^{(s)}(\boldsymbol{\kappa}))z] + \\
 & + \beta(\boldsymbol{\kappa}) \sin[\kappa_-(\boldsymbol{\kappa}, \omega_i^{(s)}(\boldsymbol{\kappa}))|z|] \} \exp[-\kappa_+(\boldsymbol{\kappa}, \omega_i^{(s)}(\boldsymbol{\kappa}))|z|],
 \end{aligned}
 \tag{9}$$

where $\alpha(\boldsymbol{\kappa})$ and $\beta(\boldsymbol{\kappa})$ are coefficients. Thus, in the regime $2B\Xi > A^2$, the function $\psi_i^{(s)}(\boldsymbol{\kappa}, z)$ away from the δ layer shows an exponential decay accompanied by an oscillation.

If the scattering is weak enough, $(aV_i/2Bk_0)^2 \ll 1$, the δ layer creates the bound states, the sub-bands $\omega_i^{(s)}(\boldsymbol{\kappa})$ of which are slightly split off from the band edges of the host,

$$\Omega - |\omega_i^{(s)}(0)| = \frac{1}{[\lambda_i^{(s)}]^2} \left[1 + \frac{\Xi}{\Omega} \right], \quad \lambda_i^{(s)} = \frac{2B}{A} \left(\frac{2Bk_0}{a|V_i|} \right), \quad (10)$$

where the corresponding localization lengths $\lambda_i^{(s)} = [\kappa_+(\omega_i^{(s)})]^{-1}$ are very long in comparison with the characteristic length $\lambda^{(A)} = 2B/A$.

Under the stipulation of the strong scattering on the δ layer, when $(aV_i/A)^2 \gg 1$, it is not difficult to one obtains analytical solutions of Eqs. (7), (8) in the form:

$$\begin{aligned} \omega_{1,2}^{(s)}(\boldsymbol{\kappa}) &= -\Xi(\boldsymbol{\kappa})(\tilde{V}_1^{-1} + \tilde{V}_2^{-1}) \pm \\ &\pm \sqrt{\Xi^2(\boldsymbol{\kappa})(\tilde{V}_1^{-1} - \tilde{V}_2^{-1})^2 + A^2\kappa^2}, \quad (11) \\ \omega_{3,4}^{(s)}(\boldsymbol{\kappa}) &= -\Xi(\boldsymbol{\kappa})(\tilde{V}_3^{-1} + \tilde{V}_4^{-1}) \pm \\ &\pm \sqrt{\Xi^2(\boldsymbol{\kappa})(\tilde{V}_3^{-1} - \tilde{V}_4^{-1})^2 + A^2\kappa^2}, \end{aligned}$$

where $\tilde{V}_i = aV_i/A$ is the dimensionless strength. These expressions are valid at $\omega^2 < \Omega^2$ and, correspondingly, $\kappa \lesssim \Omega/A$. One can see from Eq. (11), the symmetric bound states acquire the spectrum of the massive Dirac fermions, the energy shift and gap of which are proportional to $-(V \pm \eta)$ and $|\Delta \pm v|$, respectively. It is worth noting that if the effective potential (3) contains either only the matrix elements V and Δ , i.e., $V \neq 0$, $\Delta \neq 0$, and $v = \eta = 0$, these states are double degenerate, $\omega_1^{(s)}(\boldsymbol{\kappa}) = \omega_3^{(s)}(\boldsymbol{\kappa})$, $\omega_2^{(s)}(\boldsymbol{\kappa}) = \omega_4^{(s)}(\boldsymbol{\kappa})$; otherwise, there are four branches of the δ layer induced spin-polarized modes. This conclusion remains valid at any magnitude of V_i . Figure 2 demonstrates the spectrum of the bound modes $\omega_i^{(s)}(\boldsymbol{\kappa})$ in the partial situation $V = \eta = 0$ (when the confinement bands are not shifted) for two values of the scattering parameter v and at the fixed value of the exchange parameter Δ . In the limit of the infinite strength $(av/A)^2 \rightarrow \infty$, the spectrum of the bound states takes the perfect conical shape $\omega^{(s)}(\boldsymbol{\kappa}) = \pm A\kappa$ (the straight lines in Fig. 2). If $(aV_i/A)^2 \gg 1$ and $V = \eta = 0$, the decay length of the confinement mode with the spin projection $\sigma = \pm$ is given by $\lambda_\sigma^{(s)}(\boldsymbol{\kappa}) = \lambda^{(A)} \left[1 + \frac{2B\Xi(\boldsymbol{\kappa})}{a^2(v+\sigma\Delta)^2} \right]$.

4. Anti-symmetric bound states at the FM δ layer. The state with the envelope function of the

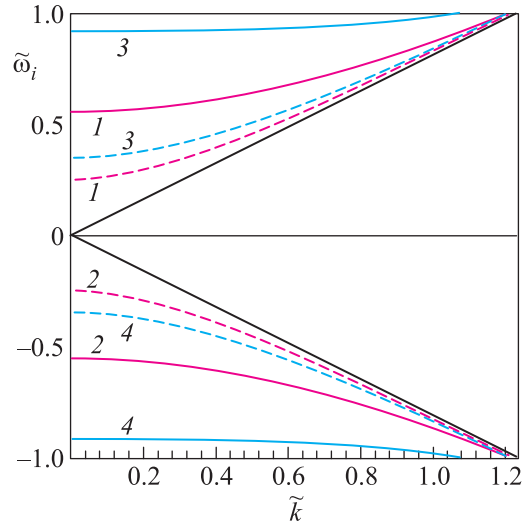


Fig. 2. (Color online) The energy spectrum of the confinement states $\omega_i^{(s)}(\mathbf{k}_{\parallel})$ in the situation $V = 0$, $v \neq 0$, $\Delta \neq 0$, $\eta = 0$ for $\tilde{\Delta} = 0.5$, $\tilde{v} = 1.0$, and $\tilde{v} = 3.0$ (dashed curves), where $\tilde{\Delta} = a\Delta/\sqrt{2B\Xi}$, $\tilde{v} = av/\sqrt{2B\Xi}$. The variables are measured in the dimensionless units: $\tilde{\omega}_i = \omega_i^{(s)}(0)/\Omega$ and $\tilde{k} = \kappa/k_0$. The curves are marked by the corresponding mode indices $i = 1, 2, 3, 4$. The linear dependence represents the spectrum of the odd state $\omega_i^{(A)}(\boldsymbol{\kappa})$

form $\psi^{(0)}(\boldsymbol{\kappa}, z) \sim \sin[(z + \phi)\sqrt{(\Omega/A)^2 - \kappa^2}] \exp(-|z + \phi|/\lambda^{(A)})$ and the Dirac spectrum $\omega^{(A)}(\boldsymbol{\kappa}) = \pm A\kappa$ is obtained with the Hamiltonian (1), (2) for the bulk TI. The state decay length $\lambda^{(A)} = 2B/A$ depends on the material parameters of the bulk TI, while the space phase ϕ is arbitrary. To obtain the envelope function of the topological surface state, Shan et al. [19] imposed the so-called open boundary condition $\psi(\boldsymbol{\kappa}, z = 0) = 0$ at the boundary of the TI-half-space with vacuum at $z = 0$. In the context of our task, to satisfy Eq. (5) at the δ layer, we choose the function $\psi^{(0)}(\boldsymbol{\kappa}, z)$ with the phase $\phi = 0$, then the expression for the spatial distribution of the antisymmetric state is given by $\psi^{(A)}(\boldsymbol{\kappa}, z) \sim \sin[z\sqrt{(\Omega/A)^2 - \kappa^2}] \exp(-|z|/\lambda^{(A)})$. The appearance of the in-gap antisymmetric bound state with the odd envelope function $\psi^{(A)}(\boldsymbol{\kappa}, z)$ and the Dirac spectrum $\omega^{(A)}(\boldsymbol{\kappa}) = \pm A\kappa$ means that the TI host loses topological invariant(s) at $z = 0$ due to the strong and local perturbation of type (3) caused by the δ layer embedded into the host. The state $\psi^{(A)}(\boldsymbol{\kappa}, z)$ is pinned up by the δ layer, but it is unaltered in form of both the envelope function and the spectrum. In this sense one can say that the state $\psi^{(A)}(\boldsymbol{\kappa}, z)$ is topologically protected similar to the topological surface state [1, 2].

Conclusion. Thus, we argue that in DMHs, wherein the δ layers are inserted into the TI host, there can appear two distinct types of the in-gap bound

states: the symmetric, $\psi^{(s)}(\boldsymbol{\kappa}, z)$, and antisymmetric, $\psi^{(A)}(\boldsymbol{\kappa}, z)$, states. The origin of the symmetric states in DMHs is in one-to-one correspondence with the origin of the convenient confinement states of carriers at interfaces or (sub)monolayers insertions in traditional semiconductor layered structures [17, 18]. Of course, the inverted band structure of the host influences the features of the symmetric state, in particular, the fact that it exists under any magnitude and sign of the potential related to the δ layer. The antisymmetric state is a close analogue of the topological surface state attributed to the Z_2 invariant of TI [1, 2]. It emerges near the δ layer, where the topological invariance is locally destroyed, and, in this manner, the antisymmetric state represents the hallmark of topological properties of the host material.

Having elucidated the peculiar features of the bound states induced by the δ layer, we propose the design concept of a spintronic device based on the magnetic proximity effect in DMHs. Let us imagine a setup consisting of a semi-infinite semiconductor-TI host (e.g., Bi_2Te_3 , Bi_2Sb_3 , Sb_2Te_3) and a metal (e.g., Mn, Fe, Cr) – rich FM δ layer inserted parallel to the free surface of the host at the distance l from the surface. We assume that in such the system there exist four symmetric states $\psi_i^{(s)}(\boldsymbol{\kappa}, z)$ associated with the gapped sub-bands $\omega_i^{(s)}(\boldsymbol{\kappa})$ and two states possessing the linear energy-momentum relation $\omega^{(A)}(\boldsymbol{\kappa}) = \pm A\kappa$ at small κ , namely, the antisymmetric state $\psi^{(A)}(\boldsymbol{\kappa}, z)$ and the topological free-surface state $\psi^{(T)}(\boldsymbol{\kappa}, z)$. For the sake of simplicity, we suppose the situation $V = \eta = 0$ and $|v| > |\Delta|$, the energy spectrum of which is shown in Fig.2. The Fermi level μ is assumed to lie within the band gap of the TI host. The electrons (holes) that populate the Dirac cones are free to move in the plane parallel to the δ layer and the TI surface, but are strongly confined in the direction perpendicular to them, forming $2D$ helical fermion gas. Due to the finite size effect [20], the tunneling between the antisymmetric bulk state $\psi^{(A)}(\boldsymbol{\kappa}, z)$ and the surface state $\psi^{(T)}(\boldsymbol{\kappa}, z)$ opens an energy gap Θ_h in the Dirac spectrum at the Γ point. The magnitude of the tunneling gap for $(Al/2B) \gg 1$ can be estimated as $\Theta_h \sim (A^2/B) \exp(-Al/2B)$ [19]. Assuming for certainty that the Fermi level lies above zero, $\mu > 0$, and intersects at least one of two confinement sub-bands with opposite spin polarizations $\sigma = \pm$ (the circumstance in which we are most interested), $\omega_1^{(s)}(\boldsymbol{\kappa}) = \omega_+^{(s)}(\boldsymbol{\kappa})$, $\omega_3^{(s)}(\boldsymbol{\kappa}) = \omega_-^{(s)}(\boldsymbol{\kappa})$, the carriers of the partially occupied states are polarized on the scale $\lambda_\sigma^{(s)}(\boldsymbol{\kappa})$ and the magnetization (i.e. short-range spin order) $m(z) \sim \sum_{\boldsymbol{\kappa}, \sigma} |\psi_\sigma^{(s)}(\boldsymbol{\kappa}, z)|^2 \hbar(\mu - \omega_\sigma^{(s)}(\boldsymbol{\kappa}))$ appears

about the FM δ layer, where $h(\omega)$ is the Heaviside function. The asymptotic behaviour of the magnetization, $m(z) \sim \exp(-2|z|/\lambda^{(s)})$, is determined by the confinement mode with smallest binding energy, $\lambda^{(s)} \sim \sim \max(\Omega - |\omega_\sigma^{(s)}(0)|)^{-1}$. We would like to emphasize that, as seen in Fig.2, the energy of electron (hole) excitation from any confinement sub-band to the bulk conduction (valence) band is always smaller than that from the Dirac band, i.e., $|\omega_i^{(s)}(\boldsymbol{\kappa})| > |\omega^{(A)}(\boldsymbol{\kappa})| = A\kappa$, therefore the penetration length of the confinement state is always longer than the penetration length of the antisymmetric state, $\lambda^{(s)} > \lambda^{(A)}$. Moreover, when the interaction of electrons with the δ layer is weak, $(a|v \pm \Delta|/2Bk_0)^2 \ll 1$, one has $\frac{\lambda^{(s)}}{\lambda^{(A)}} = \frac{2Bk_0}{a|v \pm \Delta|} \gg 1$. Thus, the confinement state induced by the FM δ layer has rather extended character along the growth axis of DMH because of its small binding energy, so it can spread over a wide enough range ($\lambda^{(s)} \approx l$) to reach the surface of the semi-infinite TI host. In such the case, the surface helical electrons, subjected to the influence of the spin-splitting exchange field normal to the surface and proportional to the build-in magnetization $m(z)$, become massive with the gap $\Theta_m \sim m(z = l)$. Remarkably, the size effect produces negligibly small gapping Θ_h compared to the exchange (time-reversal breaking) gap $\Theta_m \gg \Theta_h$. Note, the antisymmetric state also becomes massive but with larger gap $\sim m(z = 0)$.

Therein lies a feasible mechanism for “remote” control (via the FM δ layer that is separated from the surface by a TI spacer of finite thickness l) of quantum spin transport on the clean surface holding the helical electrons. The essential advantage of this mechanism in proposed DMHs is that the breaking of time-reversal symmetry and gapping of helical states on the surface are attained without direct contact with a FM insulating/metallic coating, therefore the structure saves perfectly conducting surface channel with high mobility.

We hope our speculative finding of the specific magnetic proximity effect in DMHs will stimulate the opening of an entire new playground where characters of topological materials can be experimentally studied.

-
1. M. Z. Hasan and C. L. Kane, Rev. Mod. Phys. **82**, 3045 (2010).
 2. X.-L. Qi and S.-C. Zhang, Rev. Mod. Phys. **83**, 1057 (2011).
 3. X.-L. Qi, T. L. Hughes, and S.-C. Zhang, Phys. Rev. B **78**, 195424 (2008).
 4. I. Garate and M. Franz, Phys. Rev. Lett. **104**, 146802 (2010).
 5. R. Yu, W. Zhang, H.-J. Zhang et al., Science **329**, 61 (2010).

6. T. Fujita, M. B. A. Jalil, and S. G. Tan, *Applied Physics Express* **4**, 094201 (2011).
7. Y. L. Chen, J.-H. Chu, J. G. Analytis et al., *Science* **329**, 659 (2010).
8. L. A. Wray, S.-Y. Xu, Y. Xia et al., *Nat. Phys.* **7**, 32 (2011).
9. I. Vobornik, U. Manju, J. Fujii et al., *Nano Lett.* **11**, 4079 (2011).
10. W. K. Tse and A. H. MacDonald, *Phys. Rev. Lett.* **105**, 057401 (2010).
11. K. Kawakami, E. Johnston-Halperin, L. F. Chen et al., *Appl. Phys. Lett.* **77**, 2379 (2000).
12. T. Jungwirth, J. Sinova, J. Mašek et al., *Rev. Mod. Phys.* **78**, 809 (2006).
13. Z. Zhou, Y.-J. Chien, and C. Uher, *Phys. Rev. B* **74**, 224418 (2006).
14. Z. Zhou, Y.-J. Chien, and C. Uher, *Appl. Phys. Lett.* **87**, 112503 (2005).
15. Z. Salman, E. Pomjakushina, V. Pomjakushin et al., *ArXiv: 1203.4850, cond-mat* (2012).
16. H. Zhang, C.-X. Liu, X.-L. Qi et al., *Nat. Phys.* **5**, 438 (2009); C.-X. Liu, X.-L. Qi, H. Zhang et al., *Phys. Rev. B* **82**, 045122 (2010).
17. S. Caprara, V. V. Tugushev, P. M. Echenique, and E. V. Chulkov, *Euro. Phys. Lett.* **85**, 27006 (2009); S. Caprara, V. V. Tugushev, and E. V. Chulkov, *Phys. Rev. B* **84**, 085311 (2011).
18. V. N. Men'shov, V. V. Tugushev, S. Caprara et al., *Phys. Rev. B* **80**, 035315 (2009); V. N. Men'shov, V. V. Tugushev, P. M. Echenique et al., *Phys. Rev. B* **78**, 024438 (2008).
19. W.-Y. Shan, H.-Z. Lu, and S.-Q. Shen, *New J. Phys.* **12**, 043048 (2010).
20. B. Zhou, H.-Z. Lu, R.-L. Chu et al, *Phys. Rev. Lett.* **101**, 246807 (2008).